

# A TEM and XRD Study of the Structural Changes Involved in Manganese-Based Regenerable Sorbents for Hot Coal Gas Desulfurization

L. Alonso and J. M. Palacios\*

*Instituto de Catálisis y Petroleoquímica, CSIC, Campus Universidad Autónoma, Cantoblanco, 28049 Madrid, Spain*

Received May 23, 2001. Revised Manuscript Received August 27, 2001

New technologies for power generation demand the development of regenerable sorbents for hot coal gas desulfurization down to very low levels of  $\text{H}_2\text{S}$ . Unfortunately, long-term tests in different reactors show that usual regenerable sorbents exhibit such efficiency decay and degradation of mechanical properties that their use is impractical in the current state of the art. In a previous study, some long-term tests in a fixed bed reactor have shown that Zn- or Cu-doped manganese oxide sorbents exhibit good performance. The highlighting features in the behavior of these sorbents are a substantial change in sulfidation reactivity as they are doped with zinc or copper oxides and a pronounced efficiency increase during the first 1–5 sulfidation–regeneration cycles. To understand this apparent behavior, a detailed characterization study of fresh, sulfided, and regenerated sorbents has been carried out using X-ray diffraction and transmission electron microscopy techniques. This study shows that the structure and degree of dispersion of the active phases in the fresh and regenerated sorbents and those of sulfides in the sulfided sorbents are highly dependent on the chemical nature of the dopant used. Zn enhances the formation of mixed oxide or sulfide species, while Cu increases mostly the degree of dispersion. These structural and textural changes can be associated with the high sulfidation reactivity exhibited by the studied manganese-based sorbents.

## Introduction

New technologies for an efficient and clean use of coal in power plants, such as the integrated gasification combined cycle (IGCC), are demanding the development of regenerable sorbents for gas desulfurization at high temperatures (500–800 °C) able to lower the  $\text{H}_2\text{S}$  concentration in the outlet gas from the gasifier down to a few parts per million by volume. These sorbents, generally based on metallic oxides,<sup>1</sup> usually show good performance in short-term tests in a reactor but, unfortunately, decay in long-term tests as evidenced by progressive loss of the sulfur capacity at breakthrough<sup>2</sup> and degradation of the mechanical properties<sup>3</sup> as the number of successive sulfidation–regeneration cycles increases.

Manganese oxide exhibits a high sulfidation reactivity in thermobalance tests,<sup>4</sup> and this reactivity is substantially increased by the addition of a mesoporous inert, such as alumina or bentonite.<sup>5,6</sup> One important finding in the study of these sorbents was that performance

improved with recycling during the first cycles. Its possible association, however, with the appearance and further development of some radial microcracks across the extrudate, evidenced by scanning electron microscopy (SEM), as a plausible explanation was not very convincing.<sup>7</sup> The most remarkable result in testing these sorbents was that in 14-cycle tests in a fixed bed reactor they did not show any apparent performance decay.<sup>8</sup> These results have been further confirmed in a recent study carried out with Cu-doped manganese oxides using optimized operating conditions.<sup>9</sup> Apparently, manganese sulfate, which is stable at the operating conditions under high concentrations of  $\text{SO}_2$  and  $\text{O}_2$ , can be formed in the first stages of the oxidative regeneration in a fixed bed reactor at 800 °C. However, it becomes unstable under low  $\text{SO}_2$  concentrations prevailing in the last stages of this process. Through this mechanism of formation and subsequent decomposition occurring in every cycle, sulfate manganese may operate at 800 °C as a pore-forming additive able to keep a residual porosity in the sorbent, counterbalancing the opposing and detrimental effects derived from thermal sintering. This is a plausible mechanism explaining the endurable behavior exhibited by manganese regenerable sorbents.

Unfortunately, the sulfidation of manganese oxides is thermodynamically not as favorable as that of other

\* To whom correspondence should be addressed. Phone: 34 91 585 47 87. Fax: 34 91 585 47 60. E-mail: jmp@icp.csic.es.

(1) Swisher, J. H.; Schwerdtfeger, K. *J. Mater. Eng. Perform.* **1992**, *1*, 399.

(2) Gupta, R.; Gangwal, S. K.; Jain, S. C. *Energy Fuels* **1992**, *6*, 21.

(3) Poston, J. A. *Ind. Eng. Chem. Res.* **1996**, *35*, 875.

(4) Westmoreland, P. R.; Gibson, J. B.; Harrison, D. P. *Environ. Sci. Technol.* **1977**, *11*, 488.

(5) Ben-Slimane, R.; Hepworth, M. T. *Energy Fuels* **1994**, *8*, 1175.

(6) Kwon, K. C.; Crowe, E. R.; Gangwal, S. K. *Sep. Sci. Technol.* **1997**, *32*, 775.

(7) Ben-Slimane, R.; Hepworth, M. T. *Energy Fuels* **1994**, *8*, 1184.

(8) Ben-Slimane, R.; Hepworth, M. T. *Energy Fuels* **1995**, *9*, 372.

(9) García, E.; Palacios, J. M.; Alonso, L.; Moliner, R. *Energy Fuels* **2000**, *14*, 1296.

usual sorbents, such as zinc oxides, and consequently, the achieved  $H_2S$  concentration in the outlet gas from the reactor cannot be less than 100 ppmv at the typical operating temperature of 700 °C using coal gas. To keep the equilibrium  $H_2S$  concentration low enough, manganese oxides must be doped with small concentrations of other metallic oxides, such as those of Zn or Cu, showing more favorable thermodynamics.

The sorbent reactivity is also highly affected by the chemical nature and the concentration used of zinc or copper oxides as dopants. Additionally, it has been mentioned above that the efficiency of the fresh sorbent, usually low in the first cycle, increases substantially during the first 3–5 cycles. Fresh sorbents are prepared by calcination at high temperature from a powder mixture of single oxides, and the formation of mixed oxides takes place through solid-state reaction that, frequently, becomes incomplete. However, the regenerated sorbents are formed through gas–solid reaction in the oxidative regeneration, the sulfided species being present in probably a high degree of dispersion. These factors, affecting the textural properties of the sorbent, may explain partially some of the observed differences in performance between fresh and regenerated sorbents. The other effect may be associated with the probable presence of different chemical species or differential structural changes that can be revealed through detailed characterization studies.

The different performances exhibited by fresh and regenerated sorbents have been observed previously in multicycle tests in a fixed bed reactor undertaken with zinc oxide sorbents doped with titanium oxide. Characterization studies, however, only revealed minor structural changes related to different ionic site occupations in spinel-structure compounds. Major observed changes were concerned with the textural properties of the regenerated and sulfided sorbents, and the apparent performance decay of these sorbents could be correlated with the apparent porosity decrease derived from thermal sintering accumulated during successive cycles.<sup>10</sup>

The aim of the paper is the study of the involved structural changes in fresh, sulfided, and regenerated sorbents based on manganese oxide doped with zinc or copper oxide, using X-ray diffraction (XRD) and transmission electron microscopy (TEM) as characterization techniques, derived from the different chemical natures of the dopants, the different methods used for the preparation of the fresh and regenerated sorbents, and their evolution in long-term tests in a fixed bed reactor.

## Experimental Section

Fresh sorbents were prepared from powders of pure oxides of particle size  $<5\ \mu m$  ( $MnO_2$ ,  $ZnO$ , and  $CuO$ , Merck, reagent grade). To increase the porosity of the fresh extrudates, a 5 wt % concentration of graphite as a pore-modifier additive was used. This powder mixture was subsequently homogenized in a planetary ball mill and dispersed in water to form a paste of suitable viscosity to be extruded in a syringe to cylindrical shapes 2 mm in diameter  $\times$  2 mm in height. The extrudates were softly dried overnight at 50 °C and then calcined at 950 °C for 6 h. During calcination in an oxidant atmosphere, graphite was completely removed as  $CO_2$ , leaving in the solid a permanent network of macropores that increases substan-

tially the sorbent reactivity with minor detrimental effects on the mechanical strength.<sup>11</sup> Samples are denoted MZ(1:0.1) and MC(1:0.1) with M =  $MnO_2$ , Z =  $ZnO$ , and C =  $CuO$  and the respective atomic ratios in parentheses.

For the identification of crystalline phases, powder XRD patterns were obtained in a diffractometer, Seifert 3000, using Ni-filtered  $Cu\ K\alpha$  radiation and a counting step of 0.02°. Because the inability of XRD patterns to detect chemical structures with crystal sizes below 4–5 nm, selected area electron diffraction (SAED) patterns from areas of approximately 1  $\mu m^2$  were obtained using a transmission electron microscope, JEOL JEM-2000 FX, operating in diffraction mode at an accelerating voltage of 200 kV. Samples were prepared by picking a drop from a very diluted powder dispersion in ethanol and dropping it over TEM Cu grids coated with a thin film of amorphous carbon. The textural properties of the sorbents were obtained by Hg intrusion in a Micromeritics pore sizer 9310 instrument up to a final pressure of  $2.1 \times 10^7\ Pa$ , which allowed filling of the pores down to a 3 nm diameter.

The sorbent reactivity was studied in a Setaram TA92 thermogravimetric analyzer interfaced through an analogue-to-digital converter to a computer which measured the evolution of the sample weight continuously. Sulfidations were conducted at 700 °C using 10 mg of sample and a flow rate of 200  $cm^3/min$  with a gas composed of 1 vol %  $H_2S$  and 10 vol %  $H_2$ , balance  $N_2$ .

The sorbent performance was studied in a 2.3 cm i.d. upflow fixed bed quartz reactor at atmospheric pressure and a space velocity of 6000  $h^{-1}$  (STP). Sulfidation was carried out at 700 °C using a gas, from cylinders controlled by mass flow controllers, composed of 1 vol %  $H_2S$ , 10 vol %  $H_2$ , 15 vol %  $H_2O(v)$ , 5 vol %  $CO_2$ , and 15 vol %  $CO$ , balance  $N_2$ , simulating a gas from a typical KRW fluid bed coal gasifier. Inlet and outlet gases from the reactor were analyzed by gas chromatography using DTC and FPD detectors, and the evolution of  $H_2S$  concentration through the breakthrough curves was plotted as a function of the dimensionless time  $t/t_0$ .  $t_0$  is the calculated time from sulfur mass balance to achieve complete sorbent conversion assuming that all  $H_2S$  passing through the reactor is retained in the sorbent (ideal sorbent). Sulfidation tests were stopped when the  $H_2S$  concentration in the outlet gas was higher than 2000 ppmv. Sorbent regeneration was carried out in the same reactor at 800 °C using a gas of composition 3 vol %  $O_2$  and 30 vol %  $H_2O(v)$ , balance  $N_2$ . Sorbent regeneration was considered to be complete when no  $SO_2$  was detected in the outlet gas.

## Results and Discussion

**Fresh Sorbents.** The evolution of the conversion of the fresh sorbents in a typical thermobalance sulfidation test at 700 °C is shown in Figure 1. The sorbent conversion  $x$  is defined as  $x = (W - W_0)/(W_t - W_0)$ , in which  $W_0$  is the initial sample weight,  $W$  is the sample weight at time  $t$ , and  $W_t$  is the sample weight calculated assuming all oxides in the fresh sample were converted into sulfides in the sulfided sample. The overall reactivity of sorbent MZ(1:0.1) is higher than that of sorbent MC(1:0.1) as deduced from the respective curve slopes in Figure 1. Previous studies showed that the overall sulfidation reactivity as shown in thermobalance tests is equally controlled by diffusion of the involved gases, through intraparticle pores and those of the sulfide layer just formed as sulfidation proceeds, dependent exclusively on the textural properties, and by the intrinsic reaction dependent on the chemical nature of the sorbent. A grain model with variable properties has been successfully used to predict the evolution of the

(10) Pineda, M.; Palacios, J. M.; Alonso, L.; García, E.; Moliner, R. *Fuel* **2000**, *79*, 885.

(11) Pineda, M.; Palacios, J. M.; Tomás, F.; Cilleruelo, C.; García, E.; Ibarra, J. V. *Energy Fuels* **1998**, *12*, 409.

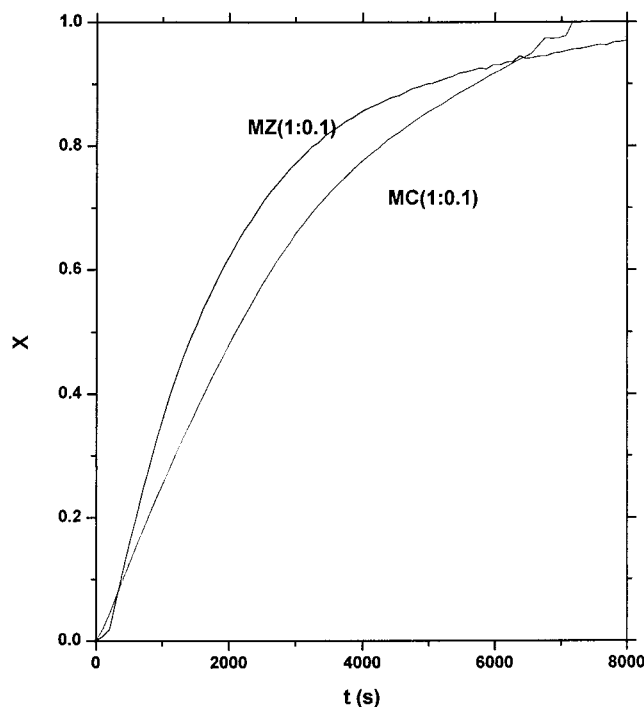


**Figure 1.** Evolution of the sulfidation conversion of the fresh sorbents MZ(1:0.1) and MC(1:0.1) in thermobalance tests.

**Table 1.** Pore Volume  $V_p$  and Surface Area  $S$  of the Fresh and Sulfided Sorbents and Reaction Constant  $k_s$  of Sulfidation

sample	$V_p$ (cm <sup>3</sup> /g)	$S$ (m <sup>2</sup> /g)	$k_s$ (m/s)
MZ(1:0.1)F	0.26	0.4	$3 \times 10^5$
MZ(1:0.1)S	0.49	1.4	
MC(1:0.1)F	0.17	0.2	$8 \times 10^6$
MC(1:0.1)S	0.40	1.2	

overall reactivity of zinc ferrites in thermobalance tests.<sup>12–14</sup> This model allows to the two different contributions to be separated, and by best fitting it is possible to determine the reaction constant  $k_s$  of the intrinsic reaction assuming for  $\text{H}_2\text{S}$  a first-order reaction.<sup>15</sup> The model uses pore volumes  $V_p$  and surface areas  $S$  of the fresh and sulfided sorbents as determined by Hg porosimetry shown in Table 1. The pore size of these sorbents is about 0.2  $\mu\text{m}$ . Because the pore volume  $V_p$  for sorbent MZ is higher than that of sorbent MC, a higher reactivity is also expected if only the role of textural properties is taken into account. It is remarkable, however, to note in Table 1 that the calculated reaction constant  $k_s$  for sorbent MZ is also considerably higher than that of sorbent MC. Both results imply not only that the degrees of dispersion of the active phases in the two fresh sorbents seem to be different but that the structures of the involved phases in the sulfidation process probably are too. Rather similar reactivities could be derived for the two sorbents if we take into account that manganese oxide is a major sorbent component, acting as a main desulfurizer agent, and

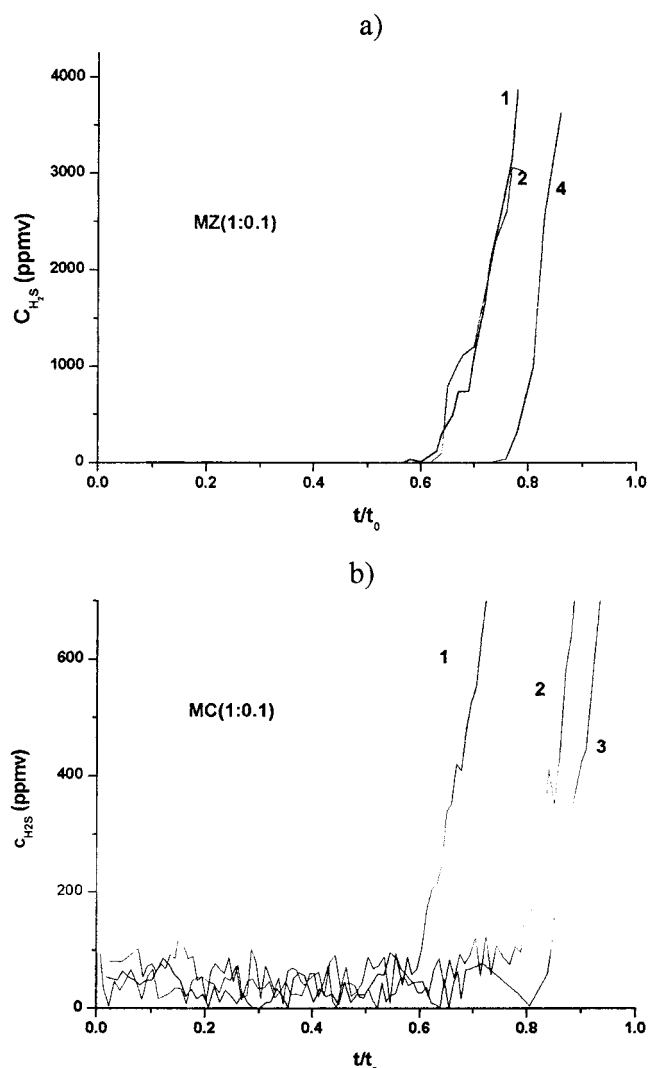


**Figure 2.** Sulfidation breakthrough curves in multicycle tests in a fixed bed reactor: (a) sorbent MZ(1:0.1); (b) sorbent MC(1:0.1).

zinc or copper oxides are dopants acting simply as polishing agents. Additionally, the two dopants show rather similar trends for the formation of mixed oxides with manganese oxide.

Differences in the overall reactivity of these sorbents are also evidenced through the respective sulfidation breakthrough curves in Figure 2 obtained in multicycle tests in a fixed bed reactor. The  $t/t_0$  ratio at breakthrough is correlated with the overall reactivity and is also a measure of the sorbent efficiency. These curves reveal that the efficiency of sorbent MZ in the first cycle is higher than that of sorbent MC, in agreement with thermobalance tests in Figure 1. The sorbent efficiency, however, increases with the number of cycles differently for the two sorbents, and in cycles 3–4 both of them show similar efficiencies. The prebreakthrough level of  $\text{H}_2\text{S}$  in the outlet gas is higher for sorbent MC (30–50 ppmv), indicating that  $\text{Cu}^{2+}$  is probably reduced to  $\text{Cu}^0$  before sulfidation takes place since the thermodynamics of  $\text{Cu}^0$  is considerably less favorable.<sup>16</sup>

From thermobalance and reactor tests it is clearly deduced that, in addition to the mentioned textural

(12) Gibson, J. B.; Harrison, D. P. *Ind. Eng. Chem. Process Des. Dev.* **1980**, *19*, 231.

(13) Ranade, P. V.; Harrison, D. P. *Chem. Eng. Sci.* **1981**, *36*, 1079.

(14) Caillet, D. A.; Harrison, D. P. *Chem. Eng. Sci.* **1982**, *37*, 625–636.

(15) Pineda, M.; Palacios, J. M.; García, E.; Cilleruelo, C.; Ibarra, J. V. *Fuel* **1997**, *76*, 567.

(16) Barin, I.; Knacke, O. *Thermochemical properties of inorganic substances*; Springer-Verlag: New York, 1973.

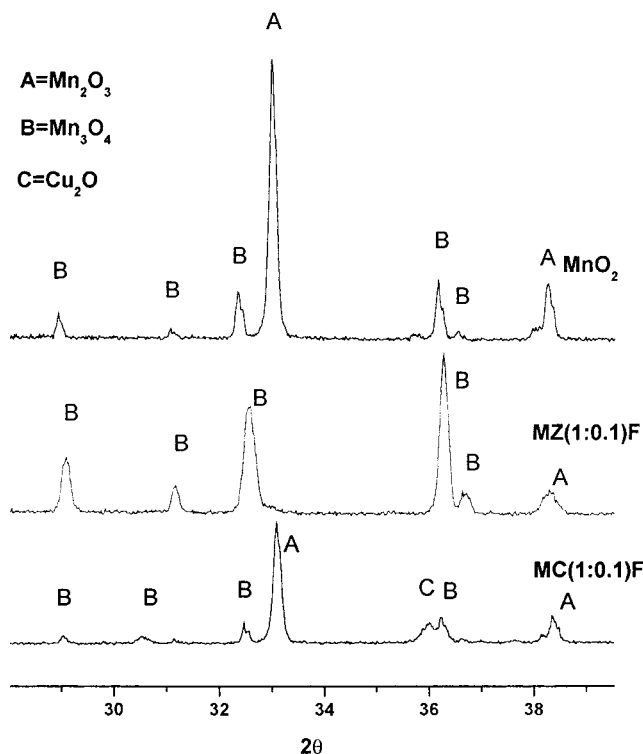


**Figure 3.** Powder X-ray patterns of the fresh sorbents calcined at 950 °C for 6 h.

changes, a 10% zinc or copper oxide doping may also induce differential structural changes in the fresh, sulfided, and regenerated sorbents of manganese-based sorbents that must be studied in detail because they can explain the different behaviors exhibited by these sorbents, especially in the first sulfidation–regeneration cycles.

The powder X-ray patterns of the fresh sorbents and that of the single oxide  $\text{MnO}_2$ , also included for comparison, all of them prepared by calcination at 950 °C for 6 h from the single powder oxides, are shown in Figure 3. The  $\text{MnO}_2$  pattern reveals the presence of  $\text{Mn}_2\text{O}_3$  (cubic) as a major phase A together with a lower concentration of  $\text{Mn}_3\text{O}_4$  (tetragonal) phase B. According to the equilibrium diagram for the system Mn–O,  $\text{MnO}_2$  should be unstable at the high temperatures of calcination, being decomposed into a mixture of  $\text{Mn}_2\text{O}_3$  and a more stable  $\text{Mn}_3\text{O}_4$ . The X-ray pattern of sorbent MC(1:0.1) is very similar to that of  $\text{MnO}_2$ , indicating that  $\text{CuO}$  doping does not affect the main structure of manganese oxide. The pattern of sorbent MZ(1:0.1), however, reveals the presence of  $\text{Mn}_3\text{O}_4$  as a major phase, indicating that  $\text{ZnO}$  doping enhances the formation of the most stable phase. Because we are dealing with a decomposition reaction, we must conclude that  $\text{ZnO}$  as dopant promotes  $\text{O}_2$  losses, which explains the higher porosity of fresh sorbent MZ as compared with that of sorbent MC, as shown in Table 1.

It is known that  $\text{Mn}_2\text{O}_3$  cannot accept dopant  $\text{CuO}$  or  $\text{ZnO}$  entering the lattice because if it does it changes rapidly to a spinel-structure compound. This phase cannot contribute to the stabilization of zinc or copper oxides, and under the strong reducing power of the coal gas they could be reduced even to the metallic state. However,  $\text{Mn}_3\text{O}_4$  can accept partial replacement of  $\text{Mn}^{2+}$  by  $\text{Cu}^{2+}$  or  $\text{Zn}^{2+}$  ions in the lattice, forming mixed oxides.

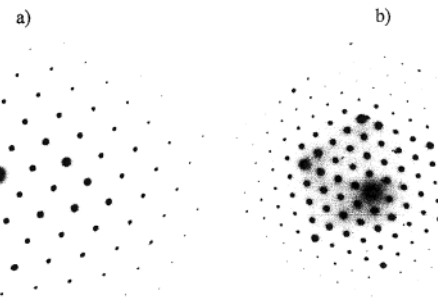


**Figure 4.** SAED patterns obtained by TEM of fresh sorbents: (a) sorbent MZ(1:0.1)F,  $\text{Mn}_3\text{O}_4$  tetragonal, zone [111]; (b) sorbent MC(1:0.1)F,  $\text{Mn}_2\text{O}_3$  cubic, zone [111].

**Table 2. Phase Concentrations in Fresh Sorbents and Lattice Parameters Calculated by Rietveld Methods**

sample	phase	c (%)	system	lattice	
				params (nm)	s (%)
$\text{MnO}_2$ calcined	$\text{Mn}_2\text{O}_3$	78	cubic	$a = 0.9405$	0.0
	$\text{Mn}_3\text{O}_4$	22	tetragonal	$a = 0.5756$ $c = 0.9467$	0.0
MZ(1:0.1)F	$\text{Mn}_3\text{O}_4$	77	tetragonal	$a = 0.5708$ $c = 0.9254$	-0.8 -2.2
	$\text{Mn}_2\text{O}_3$	23	cubic	$a = 0.9413$	0.1
	$\text{Mn}_2\text{O}_3$	81	cubic	$a = 0.9391$	-0.1
MC(1:0.1)F	$\text{Mn}_3\text{O}_4$	19	tetragonal	$a = 0.5819$ $c = 0.8655$	1.1 -8.6
	$\text{Cu}_2\text{O}$	trace			

Consequently, because single oxides,  $\text{ZnO}$  or  $\text{CuO}$ , were detected by XRD, it is deduced that dopants in both sorbents must be found inserted into the lattice of the tetragonal-phase  $\text{Mn}_3\text{O}_4$ , forming a mixed oxide. This ionic insertion might promote lattice deformations that can be assessed in a further investigation.

The concentration of the two implied phases A and B in the fresh sorbents MZ and MC and the possible deformation of the  $\text{Mn}_3\text{O}_4$  lattice due to the insertion of  $\text{Zn}$  or  $\text{Cu}$  ions have been investigated by best fitting using Rietveld methods included in the program Powder Cell v. 2.3, and the results are shown in Table 2. The effect of  $\text{ZnO}$  as a dopant is clearly evidenced through a higher concentration of the tetragonal-phase  $\text{Mn}_3\text{O}_4$  (77%) in sorbent MZ. In sorbent MC, however, the concentration of this phase is substantially lower, almost identical to that found in sorbent  $\text{MnO}_2$  taken as a reference. The dopant inclusion in the host lattice is evidenced through deformations of the respective lattice. The cubic-phase  $\text{Mn}_2\text{O}_3$  is practically unaffected by the presence of dopants, indicating that neither  $\text{Zn}$  nor  $\text{Cu}$  can enter this lattice as expected; however, the lattice of the tetragonal-phase  $\text{Mn}_3\text{O}_4$  becomes largely shrunk mostly along the  $c$ -axis, especially in  $\text{CuO}$  doping, in which case lattice deformation reaches a value of 8.6%.

Additional structural information on fresh sorbents on the microscopic scale has been gained from SAED patterns in TEM shown in Figure 4. The spots in the two patterns are clearly defined, revealing that the fresh calcined sorbents MZ and MC are made of well-crystallized compounds. The SAED pattern in sorbent MZ(1:0.1) corresponds to the tetragonal-phase  $\text{Mn}_3\text{O}_4$  zone axis [111], while the SAED pattern in sorbent MC(1:0.1) corresponds to the cubic-phase  $\text{Mn}_2\text{O}_3$  zone axis

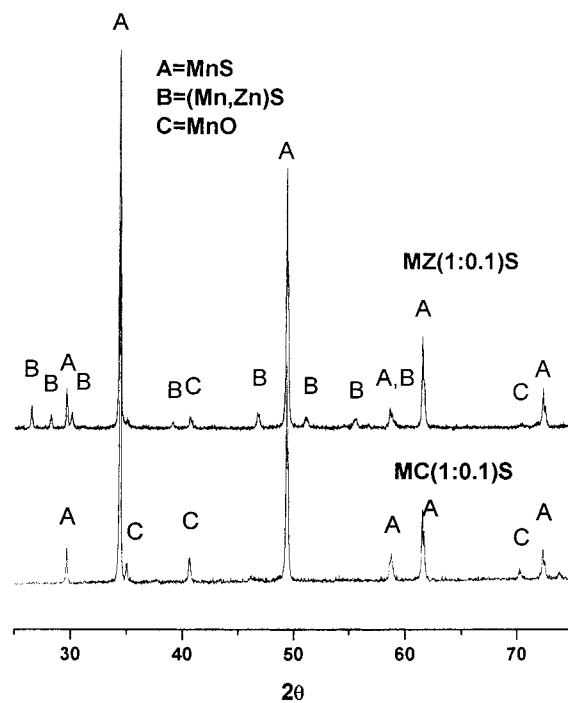


**Figure 5.** XRD patterns of sulfided sorbents MZ(1:0.1)S and MC(1:0.1)S.

**Table 3. Phase Concentration in Sulfided Sorbents and Lattice Parameters Calculated by Rietveld Methods**

sample	phase	c (%)	system	lattice	
				params (nm)	size (nm)
MZ(1:0.1)S	MnS	89	cubic	$a = 0.5219$	70
	(Mn,Zn)S	10	hexagonal	$a = 0.3882$ $c = 0.6321$	100
MC(1:0.1)S	MnO	1	cubic	$a = 0.4436$	110
	MnS	80	cubic	$a = 0.5218$	71
		20	cubic	$a = 0.4436$	25

[111]. The detected phases on the microscopic scale are in complete agreement with averaged macroscopic results obtained by XRD.

**Sulfided Sorbents.** The XRD patterns of the sulfided sorbents MZ(1:0.1)S and MC(1:0.1)S are shown in Figure 5. The two patterns reveal the presence of MnS as a major sulfided compound and traces of MnO, indicating that sorbents were not completely sulfided in the sulfidation process. Additionally, the presence of this compound indicates that under the strong reducing power of coal gas they were not stable and the initially present oxides,  $Mn_2O_3$  and  $Mn_3O_4$ , were reduced to MnO. However, the most remarkable differential feature between the two studied sorbents is the appearance in sorbent MZ of a mixed sulfide,  $(Mn,Zn)S$ , structurally similar to hexagonal ZnS but with lattice parameters very different, allowing its identification. In sorbent MC, however, the corresponding mixed sulfide was not found and the expected single copper sulfide,  $Cu_2S$ , was not detected due to, probably, poor crystallinity.

To gain quantitative information on the concentrations of different chemical species involved and their respective structures, Rietveld methods for best fitting of experimental and theoretical patterns have been applied, and the results are shown in Table 3. A higher concentration of MnO found in sorbent MC indicates a

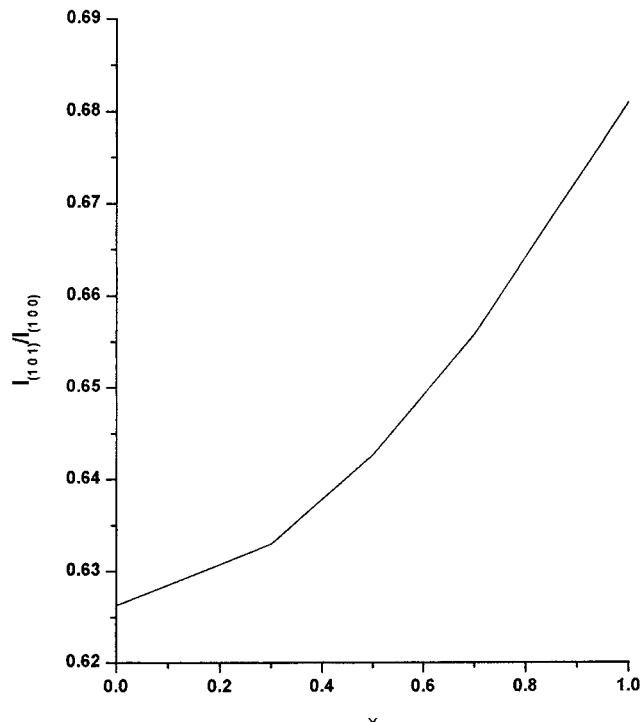


**Figure 6.** Variation of the intensity ratio  $I_{(101)}/I_{(100)}$  for simulated XRD patterns of  $(Mn_{1-x}Zn_x)S$  with different stoichiometries.

lower reactivity as compared with that of sorbent MZ, in complete agreement with fixed bed reactor (Figure 2) and thermobalance tests (Figure 1). Additionally, lattice parameters of phases MnS and MnO are not very different in the two sorbents, indicating that lattice deformations associated with the involved dopants are not found. Consequently, the most remarkable features in the sulfided sorbents shown in Table 3 are the presence of a hexagonal mixed sulfide in sorbent MZ and the small size of the crystalline domains of MnO in sorbent MC (25 nm).

It is interesting to know the stoichiometry of the mixed sulfide  $(Mn,Zn)S$  found in sorbent MZ, but unfortunately, the relatively low concentration of this compound does not allow it to be calculated directly by best fitting. It could be determined from the experimental intensity ratio  $I_{(101)}/I_{(100)}$  corresponding to the two most intense peaks in the diffractogram. For that, XRD patterns of  $(Mn_{1-x}Zn_x)S$ , in which  $x$  was varied within a broad range, have been calculated, and their respective intensity ratios are shown in Figure 6. Taking into account that the experimental intensity ratio in Figure 5 is 0.68, the corresponding value is  $x = 0.97$ . That implies that the composition of the mixed sulfide is not too far from that of the single sulfide ZnS, although the inclusion of this relatively low concentration of manganese in the sulfide lattice makes the lattice parameters change from  $a = 0.380$  nm and  $c = 0.6230$  nm corresponding to single sulfide ZnS to  $a = 0.388$  nm and  $c = 0.632$  nm for the mixed sulfide  $(Mn_{1-x}Zn_x)S$ .

The presence of this mixed sulfide in sorbent MZ(1:0.1)S and the small size of the crystalline domains of the species in sorbent MC(1:0.1)S have been further pursued by TEM, and their respective SAED patterns are shown in Figure 7. The presence of the hexagonal structure  $(Mn_{1-x}Zn_x)S$  zone [001] in sorbent MZ is

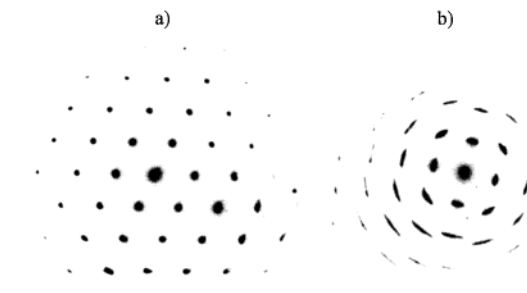


**Figure 7.** SAED patterns obtained by TEM of sulfided sorbents: (a) sorbent MZ(1:0.1)S,  $(\text{Mn}_{1-x}\text{Zn}_x)\text{S}$  hexagonal, zone [001]; (b) sorbent MC(1:0.1)S,  $\text{MnS}$  cubic, zone [001].

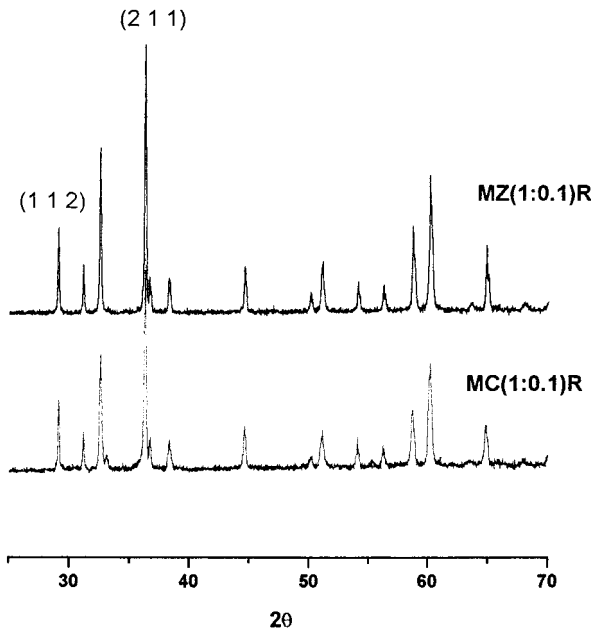


**Figure 8.** XRD patterns of regenerated sorbents MZ(1:0.1)R and MC(1:0.1)R.

clearly evidenced in Figure 7a, while the small-sized crystalline domains in sorbent MC are revealed through the slightly circularly streaked spots in the SAED pattern of cubic  $\text{MnS}$  zone [001] in Figure 7b.

**Regenerated Sorbents.** The powder XRD patterns of both regenerated sorbents MZ(1:0.1)R and MC(1:0.1)R (Figure 8) reveal the presence of the tetragonal  $\text{Mn}_3\text{O}_4$  as the only crystalline compound detected.  $\text{Mn}_2\text{O}_3$ , detected in the fresh sorbents prepared by calcination, was not found in the regenerated sorbents. Clearly, the regenerated sorbents prepared by oxidation of the sulfided sorbent behave differently than fresh sorbents, and the formation of the tetragonal phase is enhanced even at lower operating temperature (800 °C for regeneration vs 950 °C for calcination). Consequently, we can expect that fresh and regenerated sorbents also behave differently in sulfidation, which can be revealed during the first cycles in a fixed bed reactor as shown in Figure 2. The presence of a single phase implies that  $\text{Zn}^{2+}$  or  $\text{Cu}^{2+}$  ions are probably inserted into the  $\text{Mn}_3\text{O}_4$  lattice, partially replacing  $\text{Mn}^{2+}$  ions in deformed tetrahedral positions.

The results in Table 4 show that these ionic substitutions to form the mixed oxides  $(\text{Mn}_{1-x}\text{Zn}_x)\text{Mn}_2\text{O}_4$  or  $(\text{Mn}_{1-x}\text{Cu}_x)\text{Mn}_2\text{O}_4$ , respectively, take place with minor lattice straining although the size of the crystalline

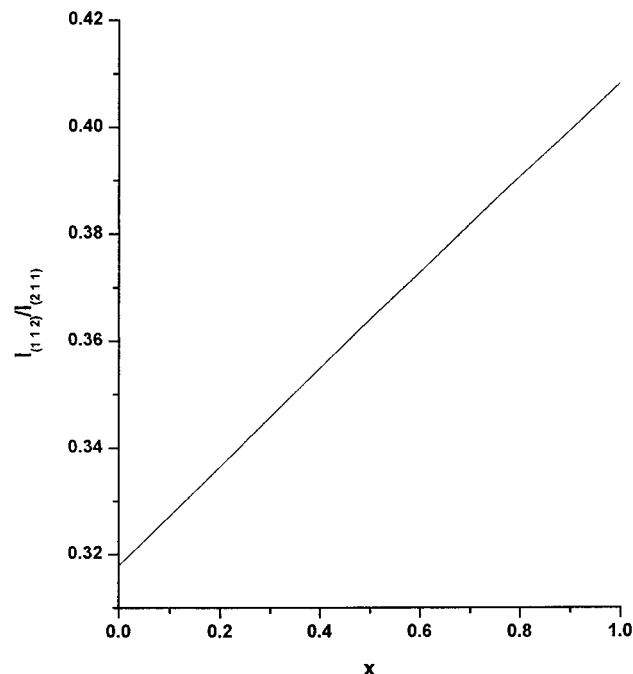


**Figure 9.** Variation of the intensity ratio  $I_{(112)}/I_{(211)}$  for simulated XRD patterns of  $(\text{Mn}_{1-x}\text{Zn}_x)\text{Mn}_2\text{O}_4$  with different stoichiometries.

**Table 4. Phase Concentration in Regenerated Sorbents and Lattice Parameters Calculated by Rietveld Methods**

sample	phase	system	lattice		
			params (nm)	<i>s</i> (%)	size (nm)
MZ(1:0.1)R	$(\text{Mn}_{1-x}\text{Zn}_x)\text{Mn}_2\text{O}_4$	tetragonal	$a = 0.5747$ $(x = 0.21)$	0.2	53
MC(1:0.1)R	$(\text{Mn}_{1-x}\text{Cu}_x)\text{Mn}_2\text{O}_4$	tetragonal	$a = 0.5761$ $(x = 0.21)$	0.1	40
			$c = 0.9410$	0.6	
			$c = 0.9426$	0.4	

domains becomes very small (40–50 nm). Another feature differentiating the fresh and regenerated sorbents is that the mixed oxides in the regenerated sorbents are found completely relaxed in a high degree of dispersion. These factors might explain the observed increase in the sorbent efficiency during the first sulfidation–regeneration cycles (Figure 2).

Further efforts have been drawn to the determination of the stoichiometric parameter  $x$  in these mixed oxides, and for that, simulated XRD powder patterns have been obtained for  $x$  varying in a broad range. The theoretical variation of the intensity ratio due to planes (112) and (211), marked in the XRD patterns in Figure 8, are shown in Figure 9. This curve is equally valid for the two mixed oxides of interest because the atomic scattering factors of Zn and Cu are very similar. The experimental intensity ratio measured from Figure 8 for the two oxides is 0.33, implying that the parameter  $x$  is about 0.21. This is approximately the expected value for  $x$  if the formation of a mixed oxide from the starting oxide concentrations is assumed. Additionally, the small size of the crystalline domains in the regenerated sorbents is shown in the respective SAED patterns. As an example, the SAED pattern from sorbent MC in Figure 10 reveals that despite the small area in which the SAED pattern was acquired a powder pattern is clearly apparent.

**Sulfided and Regenerated Sorbent MZ(1:0.1) after Long-Term Tests (70 Cycles).** Finally, the state

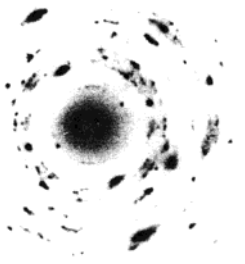


**Figure 10.** SAED pattern obtained by TEM of regenerated sorbent MC(1:0.1)R.

**Table 5. Phase Concentrations in Sulfided and Regenerated Sorbent MZ(1:0.1) after Long-Term Tests in a Fixed Bed Reactor (Cycle 70)<sup>a</sup>**

sample	phase (%)	system	lattice		
			params (nm)	<i>s</i> (%)	size (nm)
MZ(1:0.1)S	MnS	72	cubic	<i>a</i> = 0.523	0.0 61
	MnO	28	cubic	<i>a</i> = 0.444	0.1 42
MZ(1:0.1)R	Mn <sub>2</sub> O <sub>3</sub>	50	cubic	<i>a</i> = 0.942	0.0 100
	Mn <sub>3</sub> O <sub>4</sub>	50	tetragonal	<i>a</i> = 0.576 <i>c</i> = 0.931	0.4 30

<sup>a</sup> Lattice parameters were calculated using Rietveld methods.

of sorbent MZ(1:0.1) withstanding 70 successive sulfidation-regeneration cycles in a fixed bed reactor is shown in Table 5. The presence of 28% MnO in the sulfided sorbent indicates that the sorbent reactivity decreases slightly as the number of cycles increases. The lattice parameters are not substantially altered, evidenced by comparison with the data listed in Table 3, but the size of the crystalline domains of the detected species by XRD is smaller. These features indicate that the sulfidation in long-term tests in a fixed bed reactor proceeds to mainly a diffusion-controlled process of the reactant through intraparticle pores. It is also worth noting the absence of a mixed sulfide of Zn and Mn identified in the sulfided sorbent during the first cycles. SEM-EDX analysis shows that Zn is still present in the sulfided sorbent but some losses have taken place as a consequence of partial reduction of ZnO to metallic Zn and subsequent evaporation. Additionally, the corresponding sulfidation breakthrough curve correspond-

ing to cycle 70 (not shown) shows that the H<sub>2</sub>S concentration in the outlet gas from the reactor is about 3–5 ppmv, indicating that ZnO is present as a polishing agent. This apparent decrease in Zn concentration, however, probably, decreases the sensitivity limit of XRD, and consequently, (Mn,Zn)S cannot be detected. Important differential chemical changes are also apparent in the long-term regenerated sorbent. The concentration of Mn<sub>2</sub>O<sub>3</sub>, a nonexistent phase in the regenerated sorbent during the first cycles (Table 4), reaches a value of 50% in the regenerated sorbent after 70 cycles. The lattice of the supposed major phase Mn<sub>3</sub>O<sub>4</sub> is substantially shrunk mainly in the *c*-axis, indicating that diffusion problems similar to those found in the preparation of the fresh sorbents, although not as important, are apparent.

## Conclusions

To understand the different sulfidation reactivities exhibited by manganese sorbents doped with zinc or copper oxides, the increased efficiency at breakthrough revealed during the first 2–5 cycles of testing in a fixed bed reactor, and the state of the sorbents after 70 cycles in multicycle tests, a characterization study of fresh, sulfided, and regenerated sorbents has been carried out by XRD and TEM. Diffusion-controlled solid-state reactions limit the formation of the most stable oxides during calcination, making fresh sorbents structurally different from regenerated sorbents. The active phase in regenerated sorbents is also found in a higher degree of dispersion. Comparatively, zinc oxide doping enhances the formation of a tetragonal mixed oxide during calcination and a mixed sulfide during sulfidation. Copper oxide has no so relevant structural effects, but it increases substantially the degree of dispersion of sulfided and regenerated species. In long-term tests the same problems concerned with fresh sorbents appear progressively as a consequence of accumulated thermal sintering.

**Acknowledgment.** We are indebted to the European Coal and Steel Community (ECSC; Contract No. 7220-ED/093) and CICYT (Grant PPQ2000-1074) for financial support. We also acknowledge Drs. W. Kraus and G. Nolze of the Federal Institute for Materials Research Testing, Berlin, Germany, for allowing free use of the program Powder Cell v. 2.3.

CM011130P